

Solitons and deformed lattices I

B. Hartmann* and W.J. Zakrzewski†

Department of Mathematical Sciences, University of Durham,
Durham DH1 3LE, UK

Abstract

We study a model describing some aspects of the dynamics of biopolymers. The models involve either one or two finite chains with a number N of sites that represent the “units” of a biophysical system. The mechanical degrees of freedom of these chains are coupled to the internal degrees of freedom through position dependent excitation transfer functions. We reconsider the case of the one chain model discussed by Mingaleev et al. and present new results concerning the soliton sector of this model. We also give new (preliminary) results in the two chain model in which case we have introduced an interaction potential inspired by the Morse potential.

1 Introduction

Recently some work has been done on the study of curvature-induced symmetry breaking effects in nonlinear Schrödinger models [1]. The idea here is to study a one-dimensional discrete Nonlinear Schrödinger equation

$$i \frac{d}{dt} \psi_i + \sum_k J_{ik} \psi_k + \chi |\psi_i|^2 \psi_i = 0 \quad (1)$$

in which the excitation transfer function (J_{ik}) depends on the positions of the lattice points. Often [2] one restricts oneself to the nearest neighbour approximation in which case $J_{ik} = J \delta_{i-k, \pm 1}$ but, as pointed out in [1], a more general case involves $J_{ik} = J(|\vec{r}_i - \vec{r}_k|)$ where \vec{r}_i describes the spatial position of the i^{th} lattice site. Of course we expect $J(|\vec{r}_i - \vec{r}_k|)$ to be a fast decreasing function of its argument. When all the points of the lattice lie along a straight line, i.e. $\vec{r}_i = \vec{a} + \alpha_i \vec{b}$, where α_i is a linearly growing function of i , the results are not that different from the case of a regular lattice with the nearest neighbour approximation. However, as pointed out in [1], any curvature in \vec{r}_i can induce extra effects which do affect the behaviour of the ψ fields.

In [1] the authors have studied the case when the lattice points lie on a parabola with some curvature. Then they have considered $J(a)$ to be given by $J(a) = J \exp(-\alpha a)$

*e-mail address: Betti.Hartmann@durham.ac.uk

†e-mail address: W.J.Zakrzewski@durham.ac.uk

and they have showed that the effective Hamiltonian for the ψ field involves a double well potential whose shape depends on the curvature of the parabola. This has an implication on the ground states of the theory.

This idea has then been applied to the study of the dynamics of biopolymers [3]. The authors of [3] have considered the case of an excitation field ψ on a one polymer chain. The links of the polymers have been allowed to move, and their motion has been controlled by their inter-link forces and also by the force due to the excitation field ψ .

The total Hamiltonian describing the system they have considered is given by

$$H = T + U + V \quad (2)$$

where the kinetic energy T and the inter-particle interaction potential U read:

$$T = \frac{M}{2} \sum_i \left(\frac{d\vec{r}_i}{dt} \right)^2 \quad \text{and} \quad U(\vec{r}_i) = U_S + U_R + U_B . \quad (3)$$

The stretching energy U_S is given by:

$$U_S = \frac{\sigma}{2} \sum_i (|\vec{r}_i - \vec{r}_{i-1}| - a)^2 . \quad (4)$$

σ is the elastic module of the stretching rigidity of the chain and a denotes the equilibrium lattice spacing. The repulsive potential

$$U_R = \frac{\delta}{2} \sum_i \sum_{k \neq i} (d - |\vec{r}_i - \vec{r}_k|)^2 \Theta(d - |\vec{r}_i - \vec{r}_k|) \quad (5)$$

comes only into play if the distance between two particles becomes smaller than the diameter d of the particles themselves. I.e. if the particles start to overlap, they are repelled. However, since the strength δ of the repulsion is chosen finite, particles are still allowed to overlap to some extend. The final bit of the inter-particle interaction describes the bending energy:

$$U_B = \frac{\kappa}{2} \sum_i \frac{\theta_i^2}{1 - (\theta_i/\theta_{max})^2} , \quad \theta_i = \theta_i(\vec{r}_i) . \quad (6)$$

κ is the elastic module of the bending rigidity while $\theta(\vec{r}_i)$ is the angle between the two vectors $(\vec{r}_i - \vec{r}_{i-1})$ and $(\vec{r}_{i+1} - \vec{r}_i)$ (for a detailed formula see further in this paper or [3]). θ_{max} is the corresponding maximal bending angle. Finally the potential of the complex scalar field ψ reads:

$$V = \sum_i \{ 2|\psi_i|^2 - \sum_{k \neq i} J_{ik} \psi_i^* \psi_k - \frac{1}{2} \chi |\psi_i|^4 \} \quad (7)$$

where χ denotes the self-trapping nonlinearity and the excitation-transfer coefficients are given by:

$$J_{ik} = (e^\beta - 1) \exp(-\beta |\vec{r}_i - \vec{r}_k|) . \quad (8)$$

Note that the non-linear Schrödinger equation for the ψ field and the Newton equations for the chain are coupled only by the J_{ik} term.

In biophysical systems the excitation ψ_i can be thought of as an amide-I vibration, i.e. an excitation in the C=O bond of the peptide group, which transmits along the chain and deforms it. Through this interaction a new localized energy state is created, the Davydov soliton [4], which can transport energy without dispersion. Similarly, the

electron excitation on a lattice leads to a localized state called the polaron through the electron-phonon interaction [4, 5].

One end of the polymer has been set to be free; the other one, assumed to be far away, has been kept fixed.

The authors of [3] then have performed many interesting simulations of the equations which govern the dynamics of the electron and the lattice. Their most spectacular results have involved them showing that a single excitation of the ψ field at the free end results, after a long period of time, in a gradual folding of the chain. Then they have explained their results as coming from the instability generated by the development of the curvature of the chain.

These exciting results have made us think of systems involving more chains with an interchain interaction. Proteins often consist of two or more polypeptide chains and take on characteristic structures in 3-d space. Examples of such secondary structures are the α -helix and the β -sheet, where in the latter pairs of chains lie side by side being stabilised by hydrogen bonds between the carbonyl oxygen atom of one chain and the NH group of the other. Furthermore, DNA consists of two polynucleotide chains which are connected to each other by hydrogen-bonding and are coiled around each other in a double helix.

In view of these points, we have decided to extend the investigations of [3] to systems of two chains with the simplest interchain interaction as given in, e.g., [6] and inspired by the Morse potential [7]. So we have looked at a system of two chains with coupling constants given by the appropriate generalisations of those of [3]. Note that the coupling between the ψ fields on the two chains allows the field to spread between them altering the values of the effective coupling constants on each chain.

Our model is presented in the next section.

To test our program, we have, first of all, tried to reproduce the results of [3]. Unfortunately, ref [3] does not give all the details of their simulations - so in fact, not being sure what their initial conditions had been, we have not been able to reproduce their results. However, we have found some interesting properties of the system which we discuss in the following section.

Then we have looked at the system involving two chains. Our results are presented in Section 4.

We end the paper with some conclusions and our plans for the further studies.

2 Our model

As our model we take a straightforward generalisation of the model of [3] to which we have added an interaction between the chains W_{int} .

Thus the total Hamiltonian is given by :

$$H = T + U + V + W_{int} \quad (9)$$

with the kinetic energy

$$T = \sum_{j=1}^2 \frac{M_j}{2} \sum_i \left(\frac{d\vec{r}_{ij}}{dt} \right)^2, \quad (10)$$

and the inter-particle interaction:

$$U(\vec{r}_{ij}) = U_S + U_B + U_R \quad (11)$$

where the stretching energy is a sum of the respective stretching energies on chain $j = 1$ and chain $j = 2$:

$$U_S = \sum_{j=1}^2 \frac{\sigma_j}{2} \sum_i (|\vec{r}_{ij} - \vec{r}_{i-1,j}| - a_j)^2. \quad (12)$$

Similarly, the bending energy reads:

$$U_B = \sum_{j=1}^2 \frac{\kappa_j}{2} \sum_i \frac{\theta_{ij}^2}{1 - (\theta_{ij}/\theta_{max})^2}, \quad \theta_{ij} = \theta_{ij}(\vec{r}_{ij}). \quad (13)$$

Finally, the repulsive potential is a sum of the respective repulsive potentials on the two chains and a new term, which describes the repulsion if the two chains come closer than $d_{j'j}$ to each other:

$$\begin{aligned} U_R = & \sum_{j=1}^2 \left(\frac{\delta_j}{2} \sum_i \sum_{k \neq i} (d_j - |\vec{r}_{ij} - \vec{r}_{kj}|)^2 \Theta(d_j - |\vec{r}_{ij} - \vec{r}_{kj}|) \right. \\ & \left. + \sum_{j' \neq j} \frac{\delta_{j'j}}{2} \sum_i (d_{j'j} - |\vec{r}_{ij} - \vec{r}_{ij'}|)^2 \Theta(d_{j'j} - |\vec{r}_{ij} - \vec{r}_{ij'}|) \right). \end{aligned} \quad (14)$$

The energy of the excitation ψ_{ij} is given by :

$$V = \sum_{j=1}^2 \sum_i \left\{ 2|\psi_{ij}|^2 - \sum_{k \neq i} J_{ik}^j \psi_{ij}^* \psi_{kj} - \sum_{j' \neq j} \sum_l K_{il}^{jj'} \psi_{ij}^* \psi_{lj'} - \frac{1}{2} \chi_j |\psi_{ij}|^4 \right\} \quad (15)$$

with the energy transfer coefficients:

$$J_{ik}^j = \lambda_j (e^{\beta_j} - 1) \exp(-\beta_j |\vec{r}_{ij} - \vec{r}_{kj}|), \quad (16)$$

$$K_{il}^{jj'} = (e^\gamma - 1) \exp(-\gamma |\vec{r}_{ij} - \vec{r}_{lj'}|). \quad (17)$$

The second term on the rhs of (15) describes the energy transfer along one chain, while the third term corresponds to the energy transfer between the two chains.

For the interaction potential between the chains we take:

$$W_{int} = \sum_{j' \neq j} \sum_i D \{ \exp(-\alpha |\vec{r}_{ij} - \vec{r}_{ij'}|) - 1 \}^2. \quad (18)$$

The expression for the interaction potential is inspired by the Morse potential. The latter arises in a convenient model for the potential in a diatomic molecule. D then is the potential energy for the bond formation and α a parameter controlling the width of the potential well. Since the minimum of (18) is given for $\vec{r}_{ij} = \vec{r}_{ij}'$ for all i this potential leads to an attraction between the chains.

Note that our terms are simple generalisations of the expressions from [3]. All fields and coupling constants have an extra index $j = 1, 2$ which tells us which chain they refer to. We have also added a term $\sum_{j' \neq j} \sum_l K_{il}^{jj'} \psi_{ij}^* \psi_{lj'}$ coupling ψ_{ij} fields on two different chains and, as we have mentioned before, W_{int} . In addition, we have multiplied J_{ik}^j by an extra constant λ_j to extend the model to cases where the extension of the interaction over the chain and the strength of the interaction can be chosen independently from each other.

2.2 Equations

It is easy to derive equations which follow from our Hamiltonian. They are given by:

2.2.1 The Schrödinger equations

$$\begin{aligned} i \frac{\partial \psi_{ij}}{\partial t} &= 2\psi_{ij} - \sum_{k \neq i} (e^{\beta_j} - 1) \exp(-\beta_j |\vec{r}_{ij} - \vec{r}_{kj}|) \psi_{kj} \\ &- \sum_{j' \neq j} \sum_l (e^{\gamma} - 1) \exp(-\gamma |\vec{r}_{ij} - \vec{r}_{lj'}|) \psi_{lj'} \\ &- \chi_j |\psi_{ij}|^2 \psi_{ij} , \quad j = 1, 2 \end{aligned} \quad (19)$$

and, for the chains themselves:

2.2.2 The Newton equations

$$\begin{aligned} M_j \frac{d^2 \vec{r}_{ij}}{dt^2} &= -\nu_j \frac{d\vec{r}_{ij}}{dt} - \frac{dU}{d\vec{r}_{ij}} + \sum_m \sum_{k \neq m} \frac{dJ_{mk}^j}{d\vec{r}_{ij}} \psi_{mj}^* \psi_{kj} \\ &+ \sum_m \sum_{j' \neq j} \sum_l \frac{dK_{ml}^{jj'}}{d\vec{r}_{ij}} \psi_{mj}^* \psi_{lj'} - \frac{dW_{int}}{d\vec{r}_{ij}} , \quad j = 1, 2 \end{aligned} \quad (20)$$

where M_j is the mass of the particles on the j -th chain and ν_j are the corresponding damping parameters. The derivatives of the different potential terms with respect to \vec{r}_{ij} read:

$$\frac{dU_S}{d\vec{r}_{ij}} = \sigma_j \left((|\vec{r}_{ij} - \vec{r}_{i-1,j}| - a_j) \cdot \frac{\vec{r}_{ij} - \vec{r}_{i-1,j}}{|\vec{r}_{ij} - \vec{r}_{i-1,j}|} - (|\vec{r}_{i+1,j} - \vec{r}_{i,j}| - a_j) \cdot \frac{\vec{r}_{i+1,j} - \vec{r}_{i,j}}{|\vec{r}_{i+1,j} - \vec{r}_{i,j}|} \right) \quad (21)$$

$$\frac{dU_B}{d\vec{r}_{ij}} = \kappa_j \frac{\theta_{ij}}{(1 - (\theta_{ij}/\theta_{max})^2)^2} \quad (22)$$

$$\frac{dU_B}{d\vec{r}_{ij}} = -\delta_j \sum_{k \neq i} (d_j - |\vec{r}_{ij} - \vec{r}_{kj}|) \cdot \frac{\vec{r}_{ij} - \vec{r}_{kj}}{|\vec{r}_{ij} - \vec{r}_{kj}|} - \sum_{j' \neq j} \delta_{j'j} (d_{j'j} - |\vec{r}_{ij} - \vec{r}_{ij'}|) \cdot \frac{\vec{r}_{ij} - \vec{r}_{ij'}}{|\vec{r}_{ij} - \vec{r}_{ij'}|} \quad (23)$$

$$\sum_m \sum_{k \neq m} \frac{dJ_{mk}^j}{d\vec{r}_{ij}} \psi_{mj}^* \psi_{kj} = \lambda_j \beta_j (1 - e^{\beta_j}) \sum_{k \neq i} \exp\{-\beta_j |\vec{r}_{ij} - \vec{r}_{kj}|\} \cdot \frac{\vec{r}_{ij} - \vec{r}_{kj}}{|\vec{r}_{ij} - \vec{r}_{kj}|} \cdot (\psi_{ij}^* \psi_{kj} + \psi_{kj}^* \psi_{ij}) \quad (24)$$

$$\sum_m \sum_{j' \neq j} \sum_l \frac{dK_{ml}^{jj'}}{d\vec{r}_{ij}} \psi_{mj}^* \psi_{lj'} = \gamma (1 - e^\gamma) \sum_{j' \neq j} \sum_l \exp(-\gamma |\vec{r}_{ij} - \vec{r}_{lj'}|) \cdot \frac{\vec{r}_{ij} - \vec{r}_{lj'}}{|\vec{r}_{ij} - \vec{r}_{lj'}|} \cdot (\psi_{ij}^* \psi_{lj'} + \psi_{lj'}^* \psi_{ij}) \quad (25)$$

$$\frac{dW_{int}}{d\vec{r}_{ij}} = -2D\alpha \sum_{j' \neq j} \{\exp(-\alpha |\vec{r}_{ij} - \vec{r}_{ij'}|) - 1\} \cdot \frac{\vec{r}_{ij} - \vec{r}_{ij'}}{|\vec{r}_{ij} - \vec{r}_{ij'}|} \cdot \exp(-\alpha |\vec{r}_{ij} - \vec{r}_{ij'}|). \quad (26)$$

As in [3], we have introduced a viscous damping ν_j resulting from the assumption of having an aqueous environment. This is a physical reason for the introduction of such a term. On the other hand we will try to find the lowest energy (stationary) state of our system and we will use the absorption to reduce the energy and to ‘drive’ the system to its ground state. Thus, in practice, we will start with a good approximation to the ground (lowest energy) state and then evolve it with nonzero absorption - thus letting it ‘flow’ towards this true ground state.

To proceed further we need to determine the dependence of angles θ_{ij} on \vec{r}_{ij} . Geometrical reasoning gives:

$$\theta_{ij} = \pi - \tilde{\theta} \quad (27)$$

where

$$\tilde{\theta} = \arccos\left(\frac{\vec{r}_{ij}^2 - \vec{r}_{i+1,j} \cdot \vec{r}_{ij} - \vec{r}_{ij} \cdot \vec{r}_{i-1,j} + \vec{r}_{i+1,j} \cdot \vec{r}_{i-1,j}}{|\vec{r}_{ij} - \vec{r}_{i-1,j}| |\vec{r}_{i+1,j} - \vec{r}_{i,j}|}\right). \quad (28)$$

Then

$$\frac{d\theta_{ij}}{d\vec{r}_{ij}} = \left[\frac{d\theta_{ij}}{d\vec{r}_{ij}}\right]_i + \left[\frac{d\theta_{ij}}{d\vec{r}_{ij}}\right]_{i-1} + \left[\frac{d\theta_{ij}}{d\vec{r}_{ij}}\right]_{i+1} \quad (29)$$

The first term on the rhs is given by:

$$\left[\frac{d\theta_{ij}}{d\vec{r}_{ij}}\right]_i = \left(1 - \left(\frac{\vec{r}_{ij}^2 - \vec{r}_{i+1,j} \cdot \vec{r}_{ij} - \vec{r}_{ij} \cdot \vec{r}_{i-1,j} + \vec{r}_{i+1,j} \cdot \vec{r}_{i-1,j}}{|\vec{r}_{ij} - \vec{r}_{i-1,j}| |\vec{r}_{i+1,j} - \vec{r}_{i,j}|}\right)^2\right)^{-1/2} \cdot \frac{F_1(\vec{r}_{ij})}{F_2(\vec{r}_{ij})} \quad (30)$$

with

$$\begin{aligned} F_1(\vec{r}_{ij}) &= (2\vec{r}_{ij} - \vec{r}_{i+1,j} - \vec{r}_{i-1,j})(|\vec{r}_{ij} - \vec{r}_{i-1,j}| |\vec{r}_{i+1,j} - \vec{r}_{ij}|) \\ &- (\vec{r}_{ij}^2 - \vec{r}_{i+1,j} \cdot \vec{r}_{ij} - \vec{r}_{ij} \cdot \vec{r}_{i-1,j} + \vec{r}_{i+1,j} \cdot \vec{r}_{i-1,j}) \\ &\cdot \left((\vec{r}_{ij} - \vec{r}_{i-1,j}) \frac{|\vec{r}_{i+1,j} - \vec{r}_{i,j}|}{|\vec{r}_{i,j} - \vec{r}_{i-1,j}|} - (\vec{r}_{i+1,j} - \vec{r}_{ij}) \frac{|\vec{r}_{i,j} - \vec{r}_{i-1,j}|}{|\vec{r}_{i+1,j} - \vec{r}_{i,j}|}\right) \end{aligned} \quad (31)$$

and

$$F_2(\vec{r}_{ij}) = (|\vec{r}_{ij} - \vec{r}_{i-1,j}| |\vec{r}_{i+1,j} - \vec{r}_{ij}|)^2. \quad (32)$$

The second and the third terms on the rhs of (29) are given by similar expressions with functions F_3 , F_4 , and F_5 , F_6 , respectively.

We have also considered different terms to describe the effects of the curvatures of the chains. Thus we have replaced U_B by U_C :

$$U_C = \sum_{j=1}^2 \Lambda'_j \sum_i k_{ij}^2 \quad (33)$$

where k_{ij} is the curvature of the j th chain at site i and so U_C is given by

$$U_C = \sum_{j=1}^2 \Lambda_j \sum_i \left(1 - \frac{(\vec{r}_{ij} - \vec{r}_{i-1,j})(\vec{r}_{i+1,j} - \vec{r}_{ij})}{|\vec{r}_{ij} - \vec{r}_{i-1,j}| |\vec{r}_{i+1,j} - \vec{r}_{ij}|}\right) \quad (34)$$

where $\Lambda_j = 2\Lambda'_j$.

Replacing $\frac{dU_B}{d\vec{r}_{ij}}$ by $\frac{dU_C}{d\vec{r}_{ij}}$, we get:

$$\frac{dU_C}{d\vec{r}_{ij}} = \Lambda_j \left(\frac{F_1(\vec{r}_{ij})}{F_2(\vec{r}_{ij})} + \frac{F_3(\vec{r}_{ij})}{F_4(\vec{r}_{ij})} + \frac{F_5(\vec{r}_{ij})}{F_6(\vec{r}_{ij})} \right) \quad (35)$$

with F_1 etc. given by the previous equations.

Now, comparing with the expressions we have had before, we see that

$$k_{ij}^2 \propto (1 + \cos \tilde{\theta}) = (1 + \cos(\pi - \theta_{ij})) = (1 - \cos \theta_{ij}) \quad (36)$$

so that for $\theta_{ij} = 0$ (straight line), $k_{ij}^2 = 0$.

We can also introduce torsion. To do this we note that from Frenet's formulas we have

$$\tau^2 = \frac{d\vec{n}}{ds} - \kappa^2 = \frac{d^3\vec{r}}{ds^3} - \kappa^2. \quad (37)$$

Thus it would make sense to use an analog of (36) and so write

$$\tau^2 \propto (1 - \cos \phi) \quad (38)$$

where ϕ is the angle between the two planes we compare. For $\phi = 0$ it is clear that $\tau^2 = 0$. In general ϕ is given by:

$$\cos \phi = \frac{[(\vec{r}_{ij} - \vec{r}_{i-1,j}) \times (\vec{r}_{i+1,j} - \vec{r}_{ij})] \cdot [(\vec{r}_{i+1,j} - \vec{r}_{ij}) \times (\vec{r}_{i+2,j} - \vec{r}_{i+1,j})]}{\sin \theta_{ij} \sin \theta_{i+1,j} |\vec{r}_{ij} - \vec{r}_{i-1,j}| |\vec{r}_{i+1,j} - \vec{r}_{ij}|^2 |\vec{r}_{i+2,j} - \vec{r}_{i+1,j}|}. \quad (39)$$

This can be rewritten as

$$\begin{aligned} \cos \phi &= \frac{[(\vec{r}_{ij} - \vec{r}_{i-1,j}) \cdot (\vec{r}_{i+1,j} - \vec{r}_{ij})][(\vec{r}_{i+1,j} - \vec{r}_{ij}) \cdot (\vec{r}_{i+2,j} - \vec{r}_{i+1,j})]}{\sin \theta_{ij} \sin \theta_{i+1,j} |\vec{r}_{ij} - \vec{r}_{i-1,j}| |\vec{r}_{i+1,j} - \vec{r}_{ij}|^2 |\vec{r}_{i+2,j} - \vec{r}_{i+1,j}|} \\ &- \frac{[(\vec{r}_{ij} - \vec{r}_{i-1,j}) \cdot (\vec{r}_{i+2,j} - \vec{r}_{i+1,j})]}{\sin \theta_{ij} \sin \theta_{i+1,j} |\vec{r}_{ij} - \vec{r}_{i-1,j}| |\vec{r}_{i+2,j} - \vec{r}_{i+1,j}|}. \end{aligned} \quad (40)$$

We know that $\sin \theta_{ij} = \sin \tilde{\theta}_{ij}$ and that $\sin(\arccos(x)) = \sqrt{1 - x^2}$. Thus

$$\sin \theta_{ij} = \sqrt{1 - \left(\frac{\vec{r}_{ij}^2 - \vec{r}_{i+1,j} \cdot \vec{r}_{ij} - \vec{r}_{ij} \cdot \vec{r}_{i-1,j} + \vec{r}_{i+1,j} \cdot \vec{r}_{i-1,j}}{|\vec{r}_{ij} - \vec{r}_{i-1,j}| |\vec{r}_{i+1,j} - \vec{r}_{ij}|} \right)^2}. \quad (41)$$

For a straight line, we have to be careful since in Eq.(39) $\sin \theta_{ij} = 0$.

We intend to compare the effects of all these terms on the dynamics of the chains and of the excitation field. The preliminary results indicate that the dependence on the detailed form of these terms is not very strong. So in this paper we report the results for the case of U_B leaving the detailed study of the dependence on the form of U_C to a future publication. The same applies to the effects associated with non-vanishing torsion. At the same time our observation of the weak dependence on the details of U_C shows that our results are quite generic in their nature with most observed effects determined by the other terms in our Hamiltonian (2).

2.3 Initial and boundary conditions

Next we have to decide on the initial and boundary conditions.

First of all we have chosen the chains, initially, to lie parallel to each other (and we have placed them along the x axis in the xy plane, starting at $x = 0$ and running to $x = N$, where N is the total number of links of each chain). So we have put $\vec{r}_{i1}|_{t=0} = (x_{i1}, 0, 0)$, and $\vec{r}_{i2}|_{t=0} = (x_{i2}, 1, 0)$. It can then be shown that all angles vanish identically:

$$\tilde{\theta}|_{t=0} = \arccos(-1) = \pi \rightarrow \theta_{ij}|_{t=0} = 0. \quad (42)$$

It is possible to fix the ends of the chains ($x = N$) by requiring that

$$\frac{dx_{N,j}}{dt} = 0, \quad \frac{dy_{N,j}}{dt} = 0, \quad \frac{dz_{N,j}}{dt} = 0. \quad (43)$$

However, in most of our simulations, the end has been allowed to move freely.

We cannot define θ_{ij} at $x = 0$. Thus, at this point, we have taken the bending angle as the angle between the x -direction and the vector $\vec{r}_{2j} - \vec{r}_{1j}$:

$$\theta_{1j} = \arcsin(\sqrt{(y_{2j} - y_{1j})^2 + (z_{2j} - z_{1j})^2} / |\vec{r}_{2j} - \vec{r}_{1j}|). \quad (44)$$

3 One chain

In this case we have put $\sigma_2 = \kappa_2 = \delta_2 = \delta_{12} = D = \beta_2 = \gamma = \chi_2 = \nu_2 = 0$. Thus the second chain is completely decoupled and our problem is reduced to that of ref [3].

We have redone some of the work reported in [3]. We have started the simulations by putting, initially, $\psi_{1,1} = 1$ and $\psi_{i,1} = 0$, when $i = 2, \dots, N$. Using the parameters of [3], ie $\sigma_1 = 1000$, $\kappa_1 = 0.06$, $\delta_1 = 100$, $\beta_1 = 2$, $\chi_1 = 3.2$, $\nu_1 = 0.3$, $\theta_{max} = \pi/3$, $M_1 = 0.5$, $d_1 = 0.6$ and in addition $\lambda_1 = 1$, we have found that the links of the chain have moved very little, and that the motion was only in the x direction. This is easy to understand as nothing breaks the symmetry keeping the motion restricted to the $y = z = 0$ line. Of course, this symmetry can be broken dynamically through the numerical inaccuracies but this process is extremely slow.

hence we have broken the symmetry explicitly by introducing a small initial displacement of the chain in the y as well as in the z direction. Thus we put initially $y_{1,1} = 0.1$, $z_{1,1} = 0.01$ and set all other $y_{i,1}$, $z_{i,1}$ equal to zero. In all our simulations, the energy has decreased due to the absorption and has settled quite quickly to its final value.

We have first studied the existence of a soliton-like structure as a function of the parameters $\beta_1 \equiv \beta$ and λ_1 . We have found that the range of λ_1 for which the soliton doesn't get destroyed is very limited for all β_1 . For $\lambda_1 \geq 5$, $\psi_{i,1}$ is completely spread over the chain after some finite time, while for $\lambda_1 = 2, 3$, a soliton-like structure is still seen to move up and down the chain, however, a lot of "background" noise is present. A sharp soliton seems to be present only for $\lambda_1 \sim 1$. We have thus fixed $\lambda_1 \equiv 1$ and studied the dependence of the height, width and velocity of the soliton on the parameter $\beta_1 \equiv \beta$. For the position i_{max} and the height $(\psi_{i,1}\psi_{i,1}^*)_{max} = |\psi_{i,1}|_{max}^2$ of the soliton's maximum, we have used a quadratic approximation. For the width Δ of the soliton in the x -direction we can use two different definitions:

- a "quantum-mechanical" definition:

$$\Delta^{qm} = \sqrt{\langle x^2 \rangle - \langle x \rangle^2} \quad (45)$$

with $\langle x^2 \rangle = \frac{1}{N} \sum_i x_{i,1}^2 |\psi_{i,1}|^2$ and $\langle x \rangle^2 = (\frac{1}{N} \sum_i x_{i,1} |\psi_{i,1}|^2)^2$, or

- a definition using the half-maximum of $\psi\psi^*$:

$$\Delta^{1/2} = x_{1/2}^+ - x_{1/2}^- \quad (46)$$

where $x_{1/2}^+ > x_{max}$ and $x_{1/2}^- < x_{max}$ denote the two x -values for which $|\psi_{i,1}|^2(x_{1/2}^+) = |\psi_{i,1}|^2(x_{1/2}^-) = (|\psi_{i,1}|^2)_{max}/2$.

Our results for the height, position and width of the soliton as a function of $\beta_1 \equiv \beta$ after $t = 26.4$ sec are shown in Figs 1(a), (b), (c), (d) for three different values of the coupling $\chi_1 \equiv \chi$. From these figures we see that the soliton moves quicker with the decreasing of β . Moreover, the height of the soliton's maximum decreases with the decreasing of β , while at the same time the soliton gets broader as can be seen from Figs 1(c) and 1(d). Comparing Figs 1(c) and 1(d) it is also clear that the qualitative results from the two different expressions for the width are in good agreement with each other, even though the "quantum mechanical" expression takes into account all $\psi_{i,1}$ for $i \leq 40$ along the chain.

For $\beta > 10$, the excitation is completely trapped at its initial position $\psi_{1,1} = 1$. This can be explained by noting that for large β , the ψ field equation essentially decouples from the chain positions. For $\beta < 1$ it spreads over the chain with an oscillating behaviour of $|\psi_{i,1}|^2$. This is already noticeable for β s slightly larger than this value, where the soliton maximum decreases as it moves along the chain. For the reasons above, we can only calculate the maxima of the soliton etc. for the interval $\beta \in [1 : 10]$.

It had already been noticed in [3] that the soliton exists only for $2.5 < \chi < 3.5$. We find the same in our simulations with the initial excitation being trapped at its initial position for $\chi > 3.5$ and being completely destroyed for $\chi < 2.5$. Thus we have chosen $\chi = 2.8$, $= 3.0$ and $= 3.2$ to investigate the dependence on this parameter. Clearly, as seen from Fig. 1(a), the soliton moves faster as χ decreases. Moreover, its height decreases

with decreasing χ (at least comparing the results for $\chi = 3.2$ and $\chi = 2.5$). The curve for $\chi = 3.0$ is not very conclusive; however, we believe that this is due to the quadratic approximation we have used. Both methods of computing the width of the soliton again give the same qualitative result that the width decreases with increasing χ . Thus the soliton is “sharper” for larger values of χ as could have been expected.

Following [8], we have further studied the correlation between the position of the soliton and the average displacement of the site i given by :

$$\delta_{i+1} - \delta_{i-1} = \sqrt{dx_{i+1,1}^2 + dy_{i+1,1}^2 + dz_{i+1,1}^2} - \sqrt{dx_{i-1,1}^2 + dy_{i-1,1}^2 + dz_{i-1,1}^2} \quad (47)$$

where $dx_{i,1}$, $dy_{i,1}$ and $dz_{i,1}$ are the displacements from the initial position of the site i in the x , y and z directions. For two typical examples with $\chi = 3.2$, $\beta = 5$ and $\beta = 10$, respectively, with all other values given as before, we show δ_i as well as $|\psi_{i,1}|^2$ in Figs 2 (a) and 2 (b). Clearly there is a correlation between these two quantities in the sense that the maximum of $|\psi_{i,1}|^2$ is located in the region where δ_i has a local minimum. Of course, the soliton movement generates also some “background” noise which influences the displacement of the sites from their initial position. The minimum of the displacement at the left end of the chain can be attributed to the fact that we have introduced an initial displacement of the chain in both the y and z directions.

4 Two chains

We have performed several studies of a two chain system. In each case we have originally placed two chains along the $x \geq 0$ axis, one of them at $y = 0$, the other at $y = 1$ (with $z = 0$). Such a configuration does not depend on z and this symmetry is preserved by the equations of motion. Hence, to see any effects like folding, we have chosen to break the symmetry explicitly by displacing, initially, the first two links of the first chain in the z direction by: $z_{1,1} = 0.2$ and $z_{2,1} = 0.1$. We have also used other values for this displacement but we have found our results not to be too sensitive to the initial values of this displacement (as long as it was nonzero).

Then we have considered several initial conditions for the ψ_{ij} fields. In particular we have performed many simulations with $\psi_{12,1} = 1$ (and all others are zero), or with $\psi_{12,1} = 0.95$, $\psi_{13,1} = i0.3$ and all other vanishing.

We have performed these simulations for many values of β_j and χ_j . For the other parameters we have used $\sigma_1 = \sigma_2 = 3000$, $a_1 = a_2 = \kappa_1 = \kappa_2 = 1$, $\delta_1 = \delta_2 = \delta_{12} = 100$, $d_1 = d_2 = d_{12} = 0.6$ and $\gamma = 2$, $d = 0.5$, $\alpha = 1.8$.

At first this evolution is very fast, then it slows down and after a while it approaches the final configuration exponentially slowly. During the evolution at first the changes of the positions of the chains are clearly visible, then become hardly noticeable and finally the chains look as if they were essentially static. The ψ fields still evolve but even their evolution is not very dramatic. Having reached this stage we are reasonably confident that our configurations are not very different from the final asymptotic lowest energy configuration. In fact, in each case, to be absolutely certain that we are well “beyond” any transient effects, we have run each of our simulations over periods of several months

of CPU time on various SUN workstations of PCs. Thus we are ready to present our results. They are somewhat qualitative.

We have performed several simulations (for a range of values of χ_j (from 2 to 9) and for various values of β_j (from 1.5 to 2.5)).

All the simulations have shown a localised (soliton-like) behaviour of the ψ_{ij} fields, i.e. the effects on ψ_{ij} fields were reasonably well localised. This localisation concerns both chains and it depends crucially on the values of χ_j . For larger values (say $\chi_j = 6.4$) we end up with a well defined soliton-like peak (clearly visible when you add the two chains) oscillating (relatively little) in size. Like in the case of a single chain the soliton moves and its speed depends on β_j . For larger values of χ_j the soliton is narrower and so more sharply defined while for smaller values it is more spread out. For $\chi_j = 3.2$ one can still identify a clearly localised structure but whether this structure should be called a soliton remains to be decided.

We have found that the dynamics of the chains themselves depends strongly on the soliton structure. For the case of small χ_j and thus spread out $|\psi_{ij}|^2$, the chains get very much deformed (at least over short periods of time) in the sense that they have large local curvature. For sharp solitons however, i.e. large χ_j , the behaviour of the chains is very similar to that observed in the one chain model. Namely, the chains change their shape very little and remain more or less straight.

We show a typical example of the minimal energy configuration in Fig. 3. This is for $\beta_1 = \beta_2 = 2.0$ and $\chi_1 = \chi_2 = 4.0$. Note that this example corresponds to a spread out $|\psi_{ij}|^2$. Clearly, the chains have large local curvature for $0 \leq x \leq 60$. Looking at one chain by itself, it seems that loops have formed. Especially the red-coloured chain has formed a large one. Moreover, at small x , the two chains have overlapped each other in the x - y -plane and it seems like they are winding around each other. This winding also happens in the α -helix, the feature that appears e.g. in DNA.

Thus our results suggest that solitons exist when the chains are little deformed; while the large deformations of the chains correspond to more spread out $|\psi_{ij}|^2$ fields. Moreover, we have not observed any behaviour which suggests any “folding up of the chains”. At this stage our results are a little qualitative. We hope to present a more quantitative discussion of our results and an analysis of the dependence on β and κ in the next paper (sometime in the future) [9].

5 Conclusions and Outlook

In this paper we report our first results on the dynamics of biopolymer chains. While the authors of [3] put emphasis on the dynamics of a chain itself (they studied one chain) and found that for suitable choices of the coupling constants the chain folds up, we have been mainly interested in the dynamics of the soliton moving along the chain. We have found that the soliton exists only for very specific choices of the coupling constants. We have studied numerically how the speed, height and width of the soliton depend on the coupling constants. Moreover, we have confirmed the existence of a direct correlation between the

For the case of the two chain model, we have introduced suitable generalisations of the energy transfer coefficients and the rigidity potential. Moreover, we have added an attractive interaction potential between the chains inspired by the Morse potential. We have found again that the existence of the soliton depends crucially on the non-linearity parameter χ . However, while for one chain the soliton is either completely spread over the chain or sharply localised, it seems that in the case of two chains there exist a sort of intermediate situation. In this, a number of small peaks in $|\psi|^2$ exist that travel up and down the chain. Remarkably, the dynamics of the chains themselves becomes only interesting in this latter case. We find features like the formation of loops and the winding of the two chains around each other which also happens in biological systems like e.g. DNA. We plan to report a more detailed quantitative analysis of the two-chain model in a future publication [9].

6 Acknowledgement

WJZ wants to thank Y. Kivshar and S.F. Mingaleev for drawing his attention to this topic and showing him papers [1] and [3].

We also want to thank B. Piette, R. Ward, L. Brizhik and A. Eremko for their interest. BH has been supported by an EPSRC grant.

References

- [1] Yu. B. Gaididei, S. F. Mingaleev and P. J. Christiansen, *Phys. Rev. E* **62**, 2000, pp. R53-56.
- [2] see eg M. J. Ablowitz and P. A. Clarkson, *Solitons, Nonlinear Evolution Equations and Inverse Scattering*, 1991, CUP.
- [3] S. F. Mingaleev, Yu. B. Gaididei, P. J. Christiansen and Yu. S. Kivshar, *Europhys. Lett.* **59**, 2002, pp. 403-409.
- [4] A. S. Davydov, *Solitons in molecular systems*, Reidel, Dordrecht, 1985; A. Scott, *Phys. Rep.* **217**, 1992, pp. 1-67
- [5] *Nonlinear excitations in Biomolecules*, Ed.: M. Peyrard, Springer, Berlin, 1996.
- [6] M. Peyrard and A. R. Bishop, *Phys. Rev. Lett.* **62**, 1989, pp. 2755-2758; J. J. L. Ting and M. Peyrard, *Phys. Rev. E* **53**, 1996, pp. 1011-1020.
- [7] P. M. Morse, *Phys. Rev.* **34**, 1929, pp. 57-64.
- [8] P. S. Lomdahl, *Soliton models of protein dynamics in Soliton theory: a survey of results*, Ed. A. P. Fordy, Manchester University Press, 1990, pp. 209-232.
- [9] B. Hartmann and W. J. Zakrzewski, *Solitons and deformed lattices II*, in preparation.

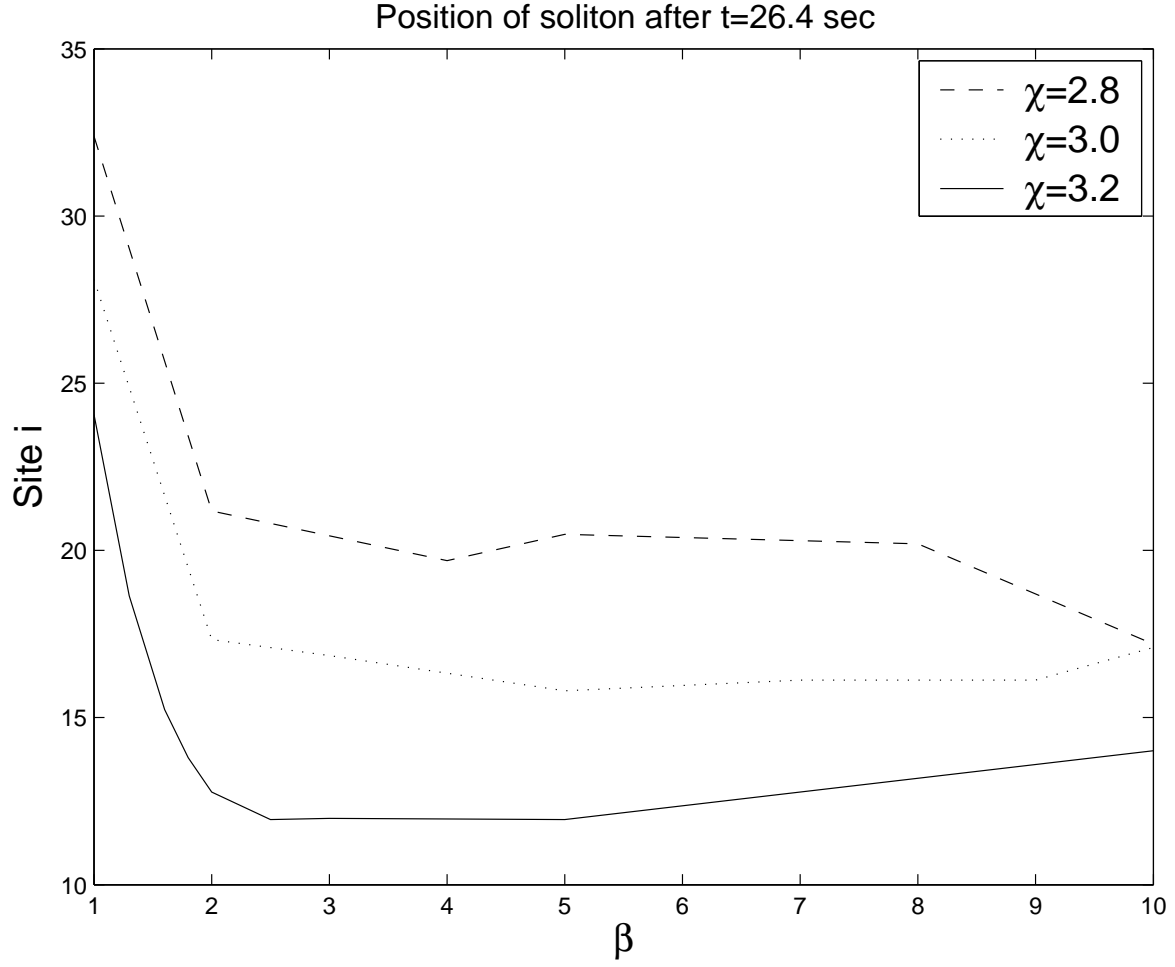


Figure 1a: The dependence of the position of the soliton's maximum at site i is shown as function of $\beta_1 \equiv \beta$ after $t = 26.4$ sec for three different values of χ .

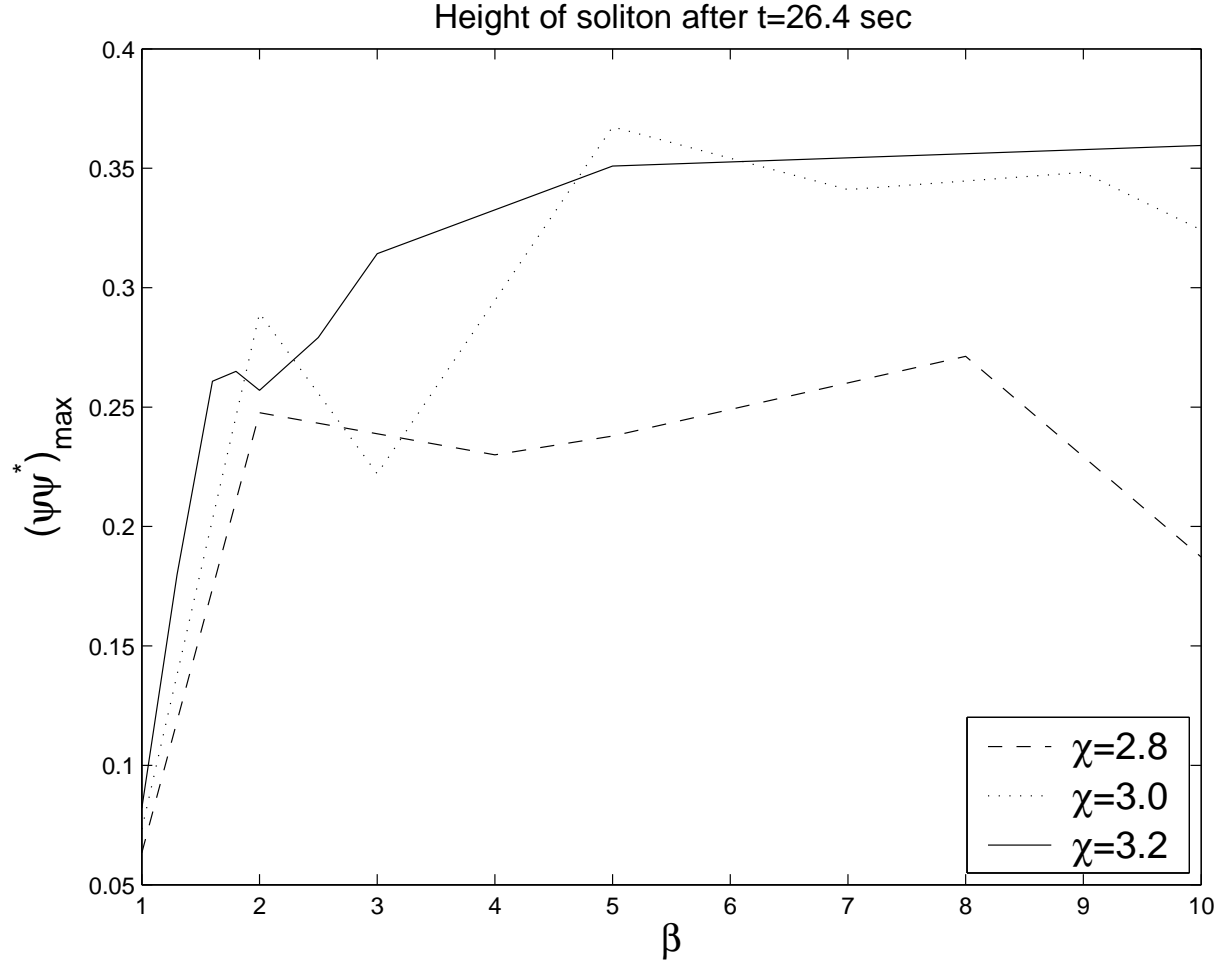


Figure 1b: The height of the soliton's maximum $(\psi\psi^*)_{\max}$ after $t = 26.4$ sec is shown as function of $\beta_1 \equiv \beta$ for three different values of χ .

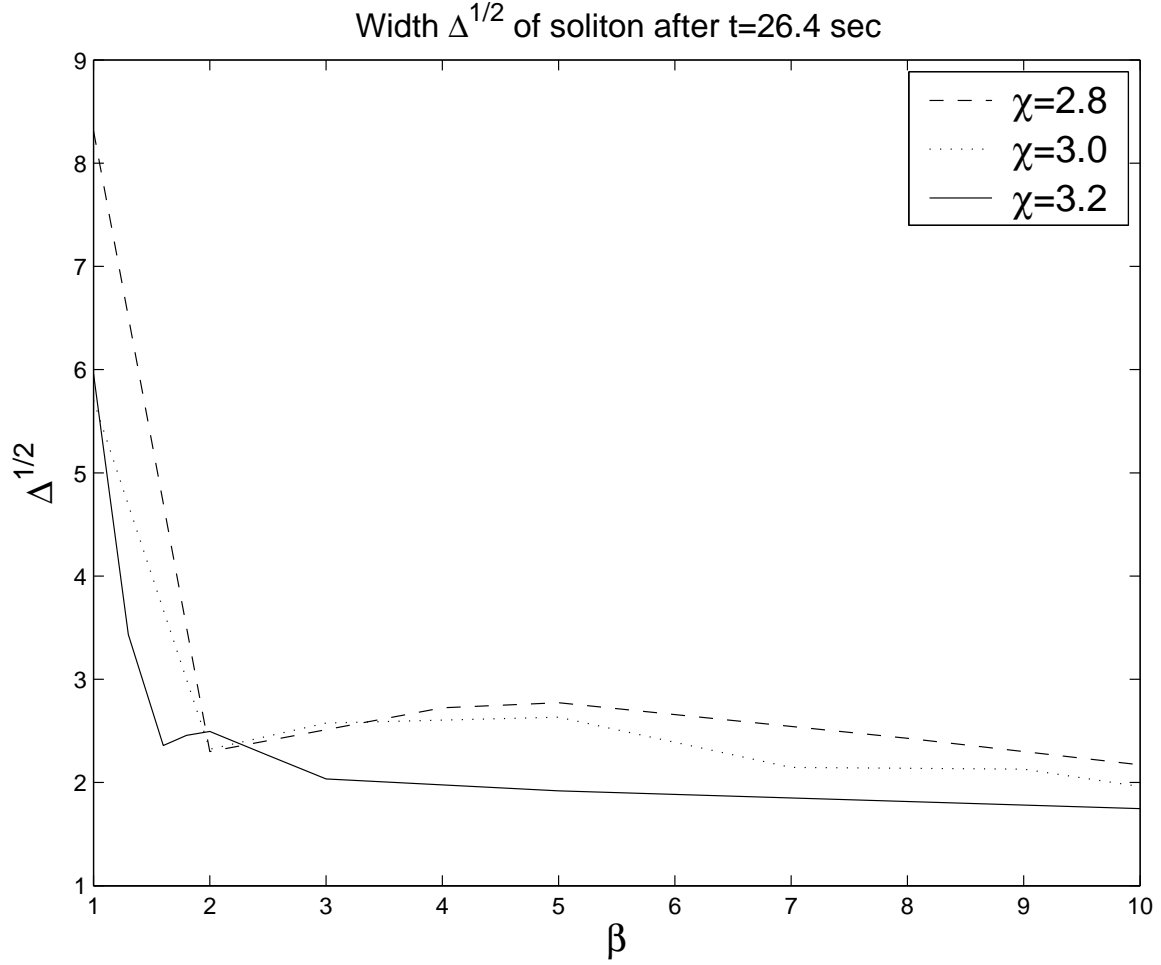


Figure 1c: The “half-maximum” width $\Delta^{1/2}$ of the soliton after $t = 26.4$ sec is given as function of $\beta_1 \equiv \beta$ for three different values of χ .

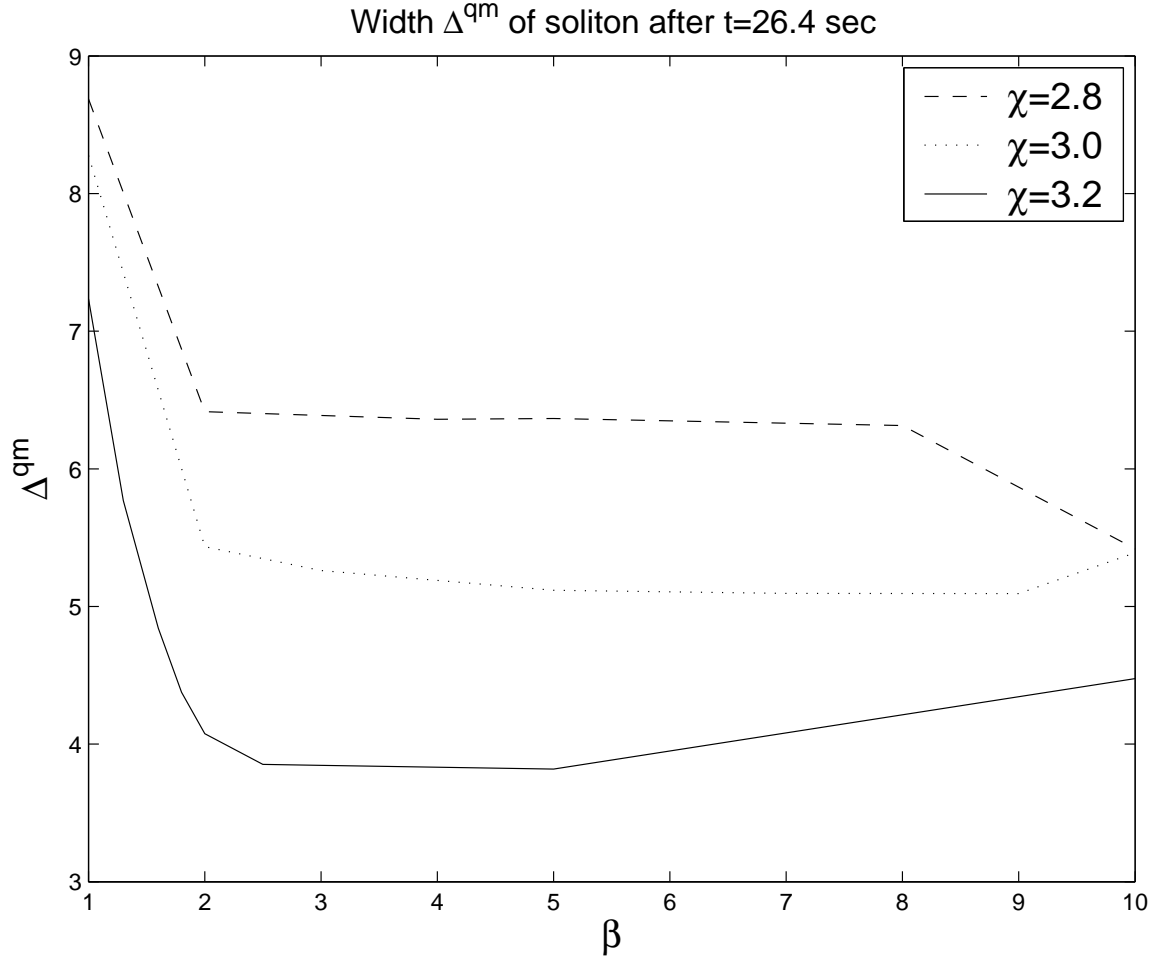


Figure 1d: The “quantum-mechanical” width Δ^{qm} of the soliton after $t = 26.4$ sec is given as function of $\beta_1 \equiv \beta$ for three different values of χ .

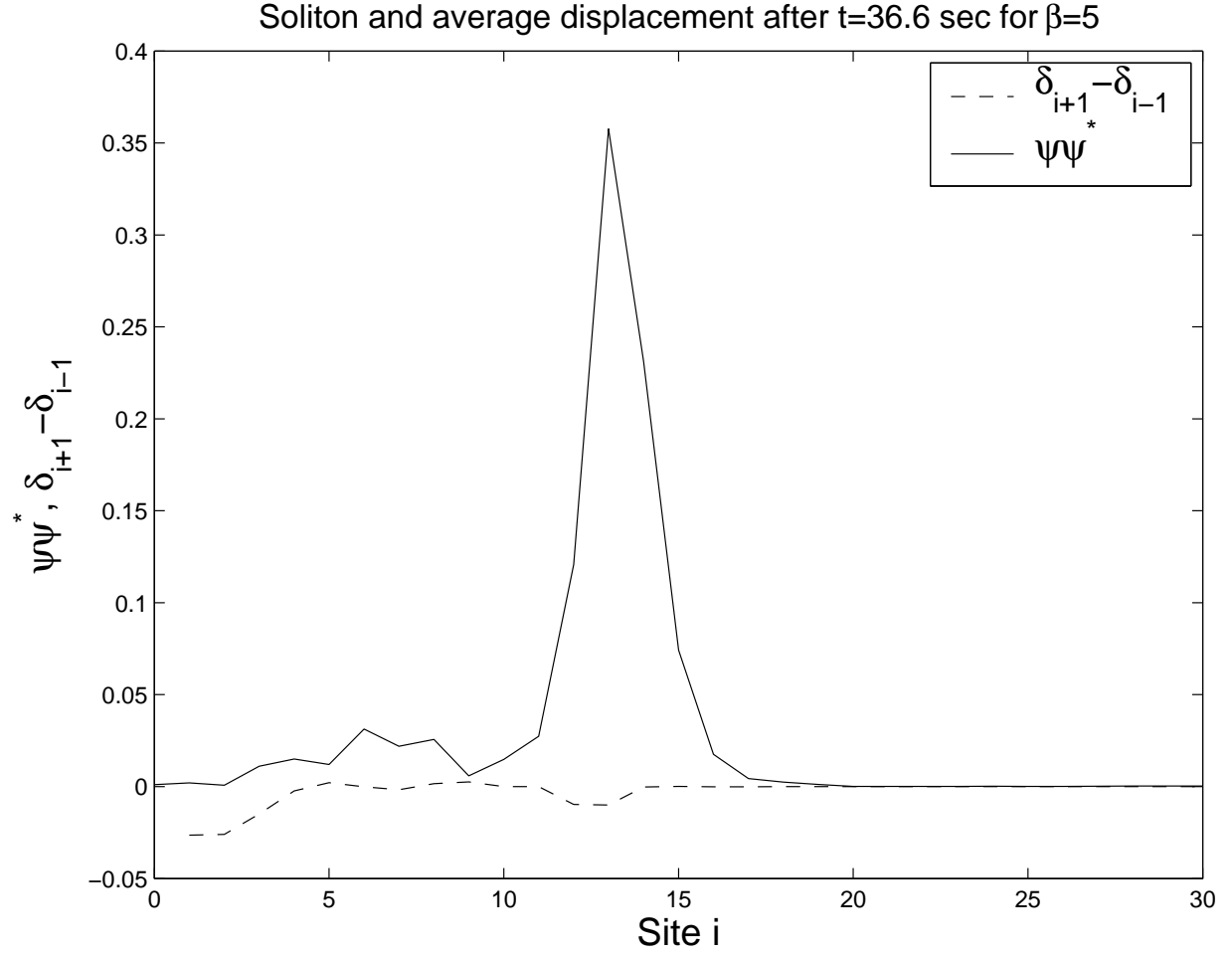


Figure 2a: The average displacement δ_i of the site i as well as $\psi_{i,1}\psi_{i,1}^* \equiv \psi\psi^*$ is shown as function of i for $\beta = 5$ after $t = 36.6$ sec.

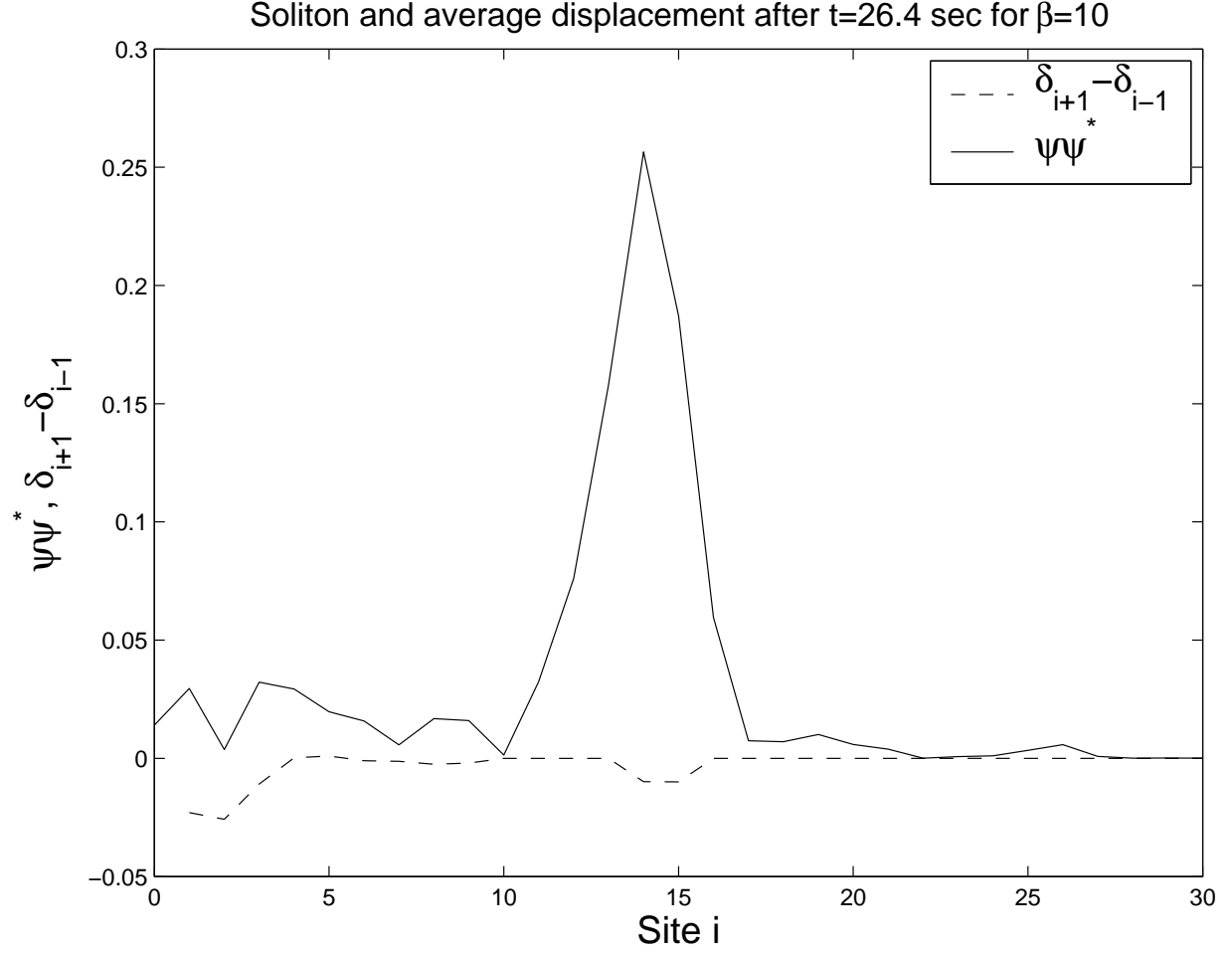


Figure 2b: The average displacement δ_i of the site i as well as $\psi_{i,1}\psi_{i,1}^* \equiv \psi\psi^*$ is shown as function of i for $\beta = 10$ after $t = 24.6$ sec.

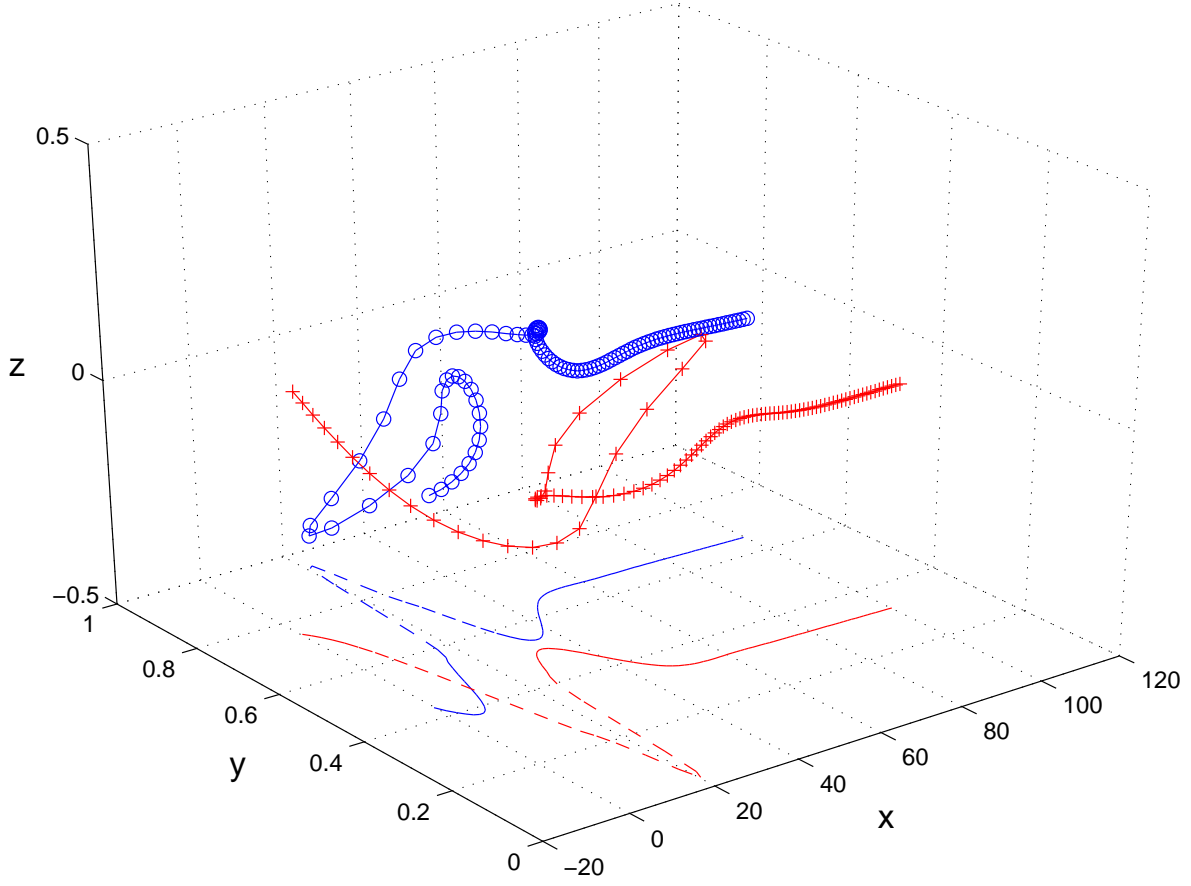


Figure 3: The minimal energy configuration of the two chains for $\beta_1 = \beta_2 = 2.0$ and $\chi_1 = \chi_2 = 4.0$ is shown in x - y - z -space. The two dashed lines at $z = -0.5$ represent the x - y -plots ($z \equiv 0$) of the chains.